DALTON
FULL PAPER

Electrochemical behaviour, IR spectroelectrochemistry and theoretical studies of tetracobalt carbonyl cluster complexes with a facial cyclooctatetraene ligand †

Jan Fiedler,[a] Carlo Nervi,[b] Domenico Osella,*[c] Maria José Calhorda,*[d,e] Sofia S. M. C. Godinho,[d] Rüdiger Merkel[f] and Hubert Wadepohl*[f]

[a] *J. Heyrovský Institute of Physical Chemistry, Academy of Sciences of the Czech Republic, Dolejškova 3, 18223 Prague 8, Czech Republic*
[b] *Dipartimento di Chimica IFM, Università di Torino, Via P. Giuria 7, 10125 Torino, Italy*
[c] *Dipartimento di Scienze e Tecnologie Avanzate, Università del Piemonte Orientale "A. Avogadro", Corso T. Borsalino 54, 15100 Alessandria, Italy. E-mail: osella@unipmn.it*
[d] *ITQB, UNL, Av. da República, Apart. 127, 2781-901 Oeiras, Portugal. E-mail: mjc@itqb.unl.pt*
[e] *Departamento de Química e Bioquímica, Faculdade de Ciências, Universidade de Lisboa, 1749-016 Lisboa, Portugal*
[f] *Anorganisch-chemisches Institut der Ruprecht-Karls-Universität, Im Neuenheimer Feld 270, D-69120 Heidelberg, Germany. E-mail: bu9@ix.urz.uni-heidelberg.de*

Received 7th June 2002, Accepted 25th July 2002
First published as an Advance Article on the web 2nd September 2002

The redox properties of some cluster complexes with a facial cyclooctatetraene (cot) ligand were investigated using electrochemical and IR spectroelectrochemical techniques. Reduction of $[Co_4(CO)_3(\mu_3\text{-}CO)_3(\mu_3\text{-}C_8H_8)L_2]$ **1** ($L_2 = \eta^4\text{-}C_8H_8$), **2** ($L_2 = \eta^4\text{-}C_6H_8$), and **3** ($L_2 = \eta^4\text{-}6,6\text{-}Ph_2C_6H_4$) occurs in CH_2Cl_2 or THF solution in two consecutive one-electron electrochemically reversible steps. Both one- and two-electron primary reduction products are unstable on a longer timescale; eventually degradation (*decapitation*) of the tetranuclear clusters takes place, to give the stable anion $[Co_3(CO)_3(\mu\text{-}CO)_3(\mu_3\text{-}C_8H_8)]^-$ **5**. The electronic structure of **1**, **2**, the octacarbonyl derivative $[Co_4(CO)_5(\mu_3\text{-}CO)_3(\mu_3\text{-}C_8H_8)]$ **4**, their monoanions, dianions and **5** was investigated using *ab initio* DFT MO calculations. The calculations showed the monoanions to be relatively stable compared to the neutral parent clusters, the relative stability depending on the type of apical ligand and reflecting its bonding capabilities, namely the possibility of ring slippage for a cot ring. Hence, an $\eta^4 \longrightarrow \eta^2$ haptotropic shift of the apical C_8H_8 ring is calculated to occur during the reduction of **1** to give the dianion $[\mathbf{1}]^{2-}$. In marked contrast, in complex **4** the haptotropic shift involves the facial, η^8-coordinated cot, which is pushed into an η^6-coordination in the optimized structure of the two-electron reduction product $[\mathbf{4}]^{2-}$. In all the cases studied, the second reduction step is however not favored energetically and reinforces the structural and electronic effects caused by the first reduction. The observed decapitation of the anionic tetranuclear cluster complexes can be traced to an ubiquitous weakening of the Co_{apical}–Co_{basal} bonds.

Introduction

Whenever the reduction of a metal cluster complex exhibits a chemically irreversible process, chemical reactions following the electron transfer often lead to a complete breakdown of the cluster.[1] The coordination of organic ligands, clasping the metallic frame in a multi-centered σ/π fashion, generally stabilizes the electro-generated ions. For instance, whereas $[Co_2(CO)_8]$ undergoes a chemically irreversible reduction, the coordination of both alkyne and diphosphane ligands, *e.g.* bis(diphenylphosphanyl)methane (dppm) in $[Co_2(CO)_4(dppm)(alkyne)]$, stabilizes the radical anion and a chemically reversible reduction is observed.[2] Recently, the chemistry of metal cluster complexes containing cycloheptatrienyl (C_7H_7, cht) and cyclooctatetraene (C_8H_8, cot) in the facial coordination mode has been reviewed.[3] The chemical properties of this class of complexes have been shown to be dominated by a high stability of the $M_3(C_nH_n)$ units.[3]

Upon chemical reduction, the tetranuclear cluster complexes $[Co_4(CO)_3(\mu_3\text{-}CO)_3(\mu_3\text{-}C_8H_8)L_2]$ **1** ($L_2 = \eta^4\text{-}C_8H_8$), **2** ($L_2 = \eta^4\text{-}C_6H_8$) and **4** (L = CO) degrade to give the trinuclear anion $[Co_3(CO)_3(\mu\text{-}CO)_3(\mu_3\text{-}C_8H_8)]^-$ **5** in quantitative yield.[4] However, preliminary cyclic voltammetry studies indicated addition of at least one electron to the tetranuclear cluster to be electrochemically reversible in most cases.[4] In contrast, after one-electron reduction the cht derivative $[Co_4(CO)_3(\mu_3\text{-}CO)_3(\mu_3\text{-}C_7H_7)(\eta^5\text{-}C_7H_9)]$ readily undergoes reversible intermolecular carbon–carbon coupling involving the 'apical' cycloheptadiene ligand, as shown by thorough chemical and electrochemical investigation.[5,6]

In the current paper we present a detailed electrochemical investigation of some tetracobalt μ_3-cot derivatives by using polarography, cyclic voltammetry (CV), exhaustive electrolysis and spectroelectrochemical techniques. Along with the electrochemical experiments *ab initio* DFT MO calculations were performed in order to characterize and understand the electronic structure and chemical behaviour of the electron-rich species formed in the primary electrode processes.

Experimental

Electrochemistry

All manipulations were carried out under argon atmosphere using Schlenk techniques. The cluster complexes were prepared

† Electronic supplementary information (ESI) available: a comparison of experimental and calculated structural parameters in clusters **1**, **2**, **4** and **5**. See http://www.rsc.org/suppdata/dt/b2/b205535j/

Table 1 Electrochemical data

Complex	$E_{1/2}$(ox)	$E_{1/2}$(0/1−)	$E_{1/2}$(1−/2−)	Solvent
$[Co_4(CO)_6(C_8H_8)_2]$ **1**	+0.32	−1.15	−1.76	CH_2Cl_2 [a]
		−0.68	−1.29	CH_2Cl_2 [b]
$[Co_4(CO)_6(C_8H_8)(C_6H_8)]$ **2**	—	−1.44	−1.88	THF [a]
		−1.02	−1.37	CH_2Cl_2 [b]
$[Co_4(CO)_6(C_8H_8)(Ph_2C_6H_4)]$ **3**	−0.04	−1.25	−2.00	THF [a]
	+0.41	−0.81	−1.48	CH_2Cl_2 [b]
$[Co_4(CO)_8(C_8H_8)]$ **4**		−0.60 [c]	−0.99 [d]	CH_2Cl_2 [b]
$[Et_4N][Co_3(CO)_6(C_8H_8)]$ $[Et_4N]^+$ **5**	−0.38	−2.45		THF [a]

[a] Potentials *vs.* $Fe(C_5H_5)_2^{0/+}$, this work. [b] Potentials *vs.* SCE, from ref. 4. [c] Semi-reversible. [d] Irreversible.

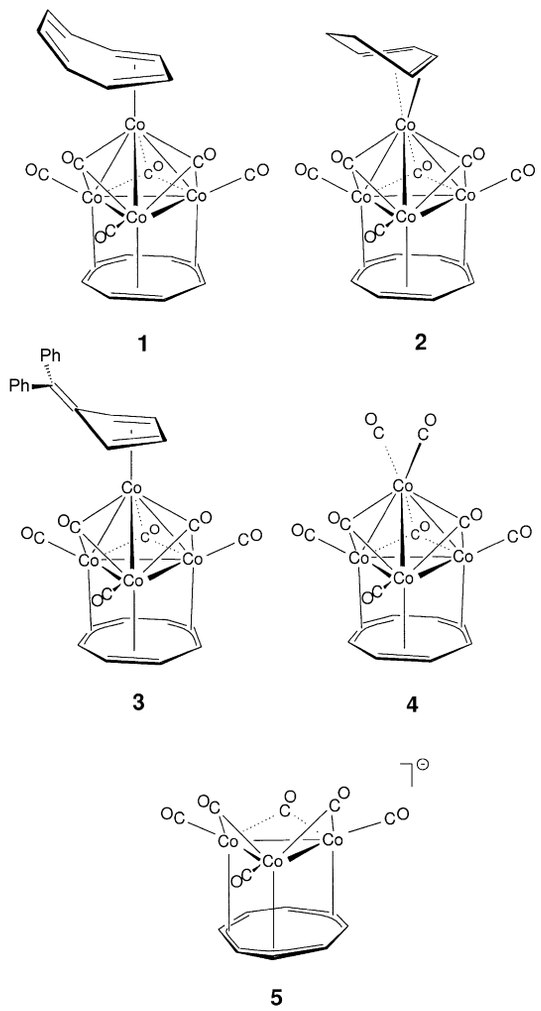

according to published procedures.[7] Electrochemistry was carried out in tetrahydrofuran (THF) or dichloromethane with tetrabutylammonium hexafluorophosphate (Bu_4NPF_6) 0.1 M as supporting electrolyte, using a standard three-electrode cell configuration (dropping mercury or glassy carbon working electrode, Pt counter electrode, SCE reference) and EG&G PAR Model 273 potentiostat. THF was distilled from sodium benzophenone immediately prior to use. Bu_4NPF_6 was obtained from the metathesis between KPF_6 (Fluka) and tetrabutylammonium iodide (Aldrich), re-crystallized three times from 95% ethanol and dried under vacuum at 110 °C overnight. We employed the ferrocene/ferrocenium couple as an internal reference. Spectroelectrochemical measurements were performed using an optically transparent thin-layer electrochemical (OTTLE) cell[8] equipped with NaCl optical windows. Time resolved infrared spectra were recorded during 5 mV s^{-1} scans, using a Bruker Equinox 55 FTIR spectrometer.

Computational details

All density functional theory calculations[9] were performed using the Amsterdam Density Functional program package (ADF).[10] The local spin density (LSD) exchange correlation potential was used with the local density approximation of the correlation energy (Vosko–Wilk–Nusair).[11] Gradient corrected geometry optimisations[12] were performed using the generalised gradient approximation (Perdew–Wang[13] exchange and correlation corrections). Spin unrestricted calculations were performed for all the paramagnetic species studied. The inner shells of Co ([1–3]s, 2p), C (1s) and O (1s) were frozen. An uncontracted triple-ζ STO basis set was used for Co 3d, 4s and 4p. The valence shells for C and O (2s, 2p) were described by an uncontracted triple-ζ STO basis set, augmented by two polarisation functions (3d and 4f). For H an uncontracted triple-ζ STO basis set (1s) with two polarisation functions 2p and 3d was used. Full geometry optimisations were performed without any symmetry constraints. The starting geometries were modelled after the crystal structures for **1**,[7] **2**,[7] **4**[7] and **5**.[4] Graphical representations of molecular orbitals were drawn with MOLEKEL.[14]

Results

Electrochemistry

Polarographic responses of the complexes $[Co_4(CO)_3(\mu_3\text{-}CO)_3(\mu_3\text{-}C_8H_8)(\eta^4\text{-}C_8H_8)]$ **1**, $[Co_4(CO)_3(\mu_3\text{-}CO)_3(\mu_3\text{-}C_8H_8)(\eta^4\text{-}C_6H_8)]$ **2** and $[Co_4(CO)_3(\mu_3\text{-}CO)_3(\mu_3\text{-}C_8H_8)(\eta^4\text{-}6,6\text{-}Ph_2C_6H_4)]$ **3**, in THF or CH_2Cl_2 solutions are all characterized by two subsequent one-electron reversible reductions (Fig. 1, Table 1). The 60 mV

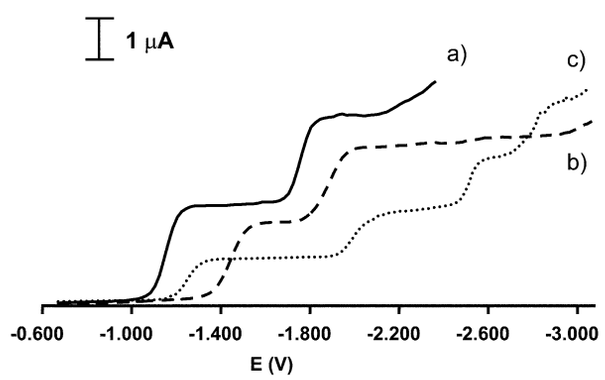

Fig. 1 Polarography of (a): 1.0 mM $[Co_4(CO)_6(C_8H_8)_2]$ **1** in CH_2Cl_2/0.1 M Bu_4NPF_6; (b): 1.0 mM $[Co_4(CO)_6(C_8H_8)(C_6H_8)]$ **2** in THF/0.1 M Bu_4NPF_6; (c): 0.5 mM $[Co_4(CO)_6(C_8H_8)(Ph_2C_6H_4)]$ **3** in THF/0.1 M Bu_4NPF_6. Potentials in V *vs.* $[Fe(C_5H_5)_2]^{+/0}$.

slopes of the logarithmic plots of the polarographic waves prove the electrochemical reversibility, and the controlled potential coulometry shows a consumption of one electron per molecule.

Complex **3** exhibits further waves in the negative cathodic region (Fig. 1c), which can be ascribed to reduction of products

formed after the decomposition of the unstable dianion. The wave at −2.5 V was identified as reduction of $[Co_3(\mu\text{-}CO)_3(CO)_3(\mu_3\text{-}C_8H_8)]^-$ **5** by comparison with an authentic sample of the salt $[Et_4N]^+$**5**, synthesized by chemical reduction of **1** with $LiHBEt_4$.[4] The bis-cyclooctatetraene cluster **1** is unstable in THF even in its neutral form and therefore the electrochemical measurements were performed in CH_2Cl_2 solutions. Irreversible oxidation waves detected at potentials +0.32 V (multielectron) and −0.04 V (monoelectron) for **1** and **3** respectively, are connected to cluster degradation and were not further investigated.

Cyclic voltammetry (Fig. 2) performed with scan rates in the

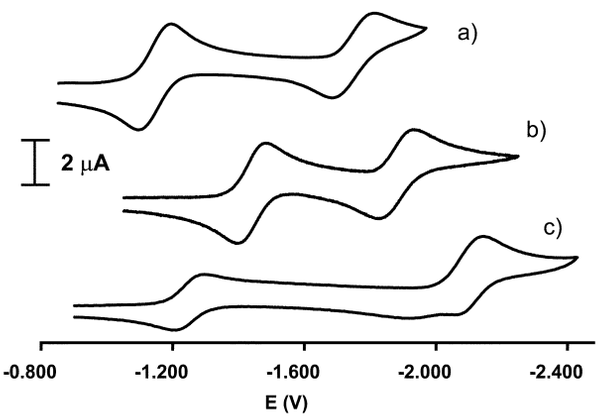

Fig. 2 Cyclic voltammograms of (a): 1.0 mM $[Co_4(CO)_6(C_8H_8)_2]$ **1** in CH_2Cl_2/0.1 M Bu_4NPF_6; (b): 1.0 mM $[Co_4(CO)_6(C_8H_8)(C_6H_8)]$ **2** in THF/0.1 M Bu_4NPF_6; (c): 0.5 mM $[Co_4(CO)_6(C_8H_8)(Ph_2C_6H_4)]$ **3** in THF/0.1 M Bu_4NPF_6 at 200 mV s^{-1} scan rate. Potentials in V *vs.* $[Fe(C_5H_5)_2]^{+/0}$.

range from 0.05 to 50 V s^{-1} shows chemically and electrochemically reversible reductions with i_p^a/i_p^c *ca.* 1 and $E_p^c - E_p^a$ *ca.* 60 mV.

The highest scan rates (around 50 V s^{-1}) reveal electrochemical quasi-reversibility (increasing anodic to cathodic peak separation due to a slow electrode transfer) in the second reduction step. In the case of the CV response of complex **3**, the anodic counterpeak at the second step is smaller and an additional peak appears in the reverse scan suggesting the decomposition of the reduced complex (Fig. 2c).

Bulk electrolysis on a mercury pool electrode at the potential of the first reduction wave leads to formation of the oxidation and reduction waves (by means of *in situ* polarography) corresponding to original first and second reduction waves, in agreement with an EE reduction mechanism. However, on a longer timescale the waves assigned to the reoxidation of $[\mathbf{1}]^-$ and $[\mathbf{3}]^-$ disappear, proving moderate chemical stability of these anions in solution. The polarographic response indicates that both $[\mathbf{1}]^-$ and $[\mathbf{3}]^-$ eventually decompose to give the trinuclear anion **5** as the final product.

Spectroelectrochemistry

Fig. 3 shows the spectral changes in the region of carbonyl stretching frequencies during the *in situ* reduction in the OTTLE cell. As expected, both terminal and bridging carbonyl stretching bands are shifted to lower frequencies upon reduction of the neutral clusters.

The process at the first reduction step is reversible and the original spectrum is restored by reoxidation. The chemical reversibility is however not complete in the case of the system **1**/$[\mathbf{1}]^-$ which in the timescale of the OTTLE measurement partially decomposes to give the anion **5**, identified by comparison of the additional bands with the spectrum of pure $[Et_4N]^+$**5**. The second reduction step leads to total decomposition of the bis-cyclooctatetraene system. The cluster **3** is slightly more stable, and the spectra of $[\mathbf{3}]^{2-}$ can be observed (Table 2) upon

Table 2 CO stretching band maxima from IR spectroelectrochemistry[a]

Complex	ν_{CO}/cm^{-1}
$[Co_4(CO)_6(C_8H_8)_2]$ **1**	2017sh, 1995, 1740sh, 1730
$[Co_4(CO)_6(C_8H_8)_2]^-$ $[\mathbf{1}]^-$	1939, 1667
$[Co_4(CO)_6(C_8H_8)(C_6H_8)]$ **2**	2014sh, 1989, 1747sh, 1726
$[Co_4(CO)_6(C_8H_8)(C_6H_8)]^-$ $[\mathbf{2}]^-$	1964sh, 1936, 1700sh, 1670
$[Co_4(CO)_6(C_8H_8)(C_6H_8)]^{2-}$ $[\mathbf{2}]^{2-}$	1877, 1637
$[Co_4(CO)_6(C_8H_8)(Ph_2C_6H_4)]$ **3**	2017sh, 1996, 1723
$[Co_4(CO)_6(C_8H_8)(Ph_2C_6H_4)]^-$ $[\mathbf{3}]^-$	1973sh, 1945,1668
$[Co_4(CO)_6(C_8H_8)(Ph_2C_6H_4)]^{2-}$ $[\mathbf{3}]^{2-}$	1900, 1862,1615[b]
$[Et_4N][Co_3(CO)_6(C_8H_8)]$ $[Et_4N]^+$ **5**	1977, 1939, 1783, 1744

[a] In 1,2-dichloroethane/0.1 M Bu_4NPF_6. [b] Very weak, poorly distinguished.

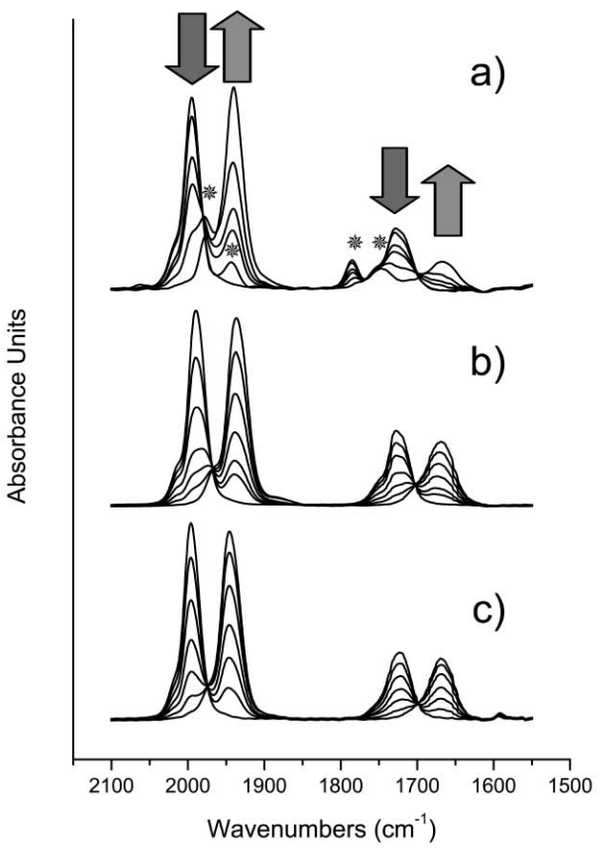

Fig. 3 IR spectroelectrochemistry. Reduction (a): **1** ⟶ $[\mathbf{1}]^-$, absorption peaks marked with stars (☆) belong to $[Co_3(CO)_6(C_8H_8)]^-$ **5**, assigned by comparison with a pure sample of $[Et_4N]^+$**5** (b): **2** ⟶ $[\mathbf{2}]^-$, (c): $[\mathbf{3}]$ ⟶ $[\mathbf{3}]^-$ in 1,2-dichloroethane/0.1 M Bu_4NPF_6.

the second reduction $[\mathbf{3}]^-/[\mathbf{3}]^{2-}$, although in a mixture with a smaller amount of **5**. The two-electron reduction product of **2** shows a higher stability. This is in agreement with the polarographic responses outlined above, where the reduction wave at −2.5 V typical of **5** appears during polarography of a solution of **3**, but not in the case of **2** (Fig. 1).

DFT studies

Full geometry optimizations of the neutral clusters $[Co_4(CO)_3(\mu_3\text{-}CO)_3(\mu_3\text{-}C_8H_8)(\eta^4\text{-}C_8H_8)]$ **1**, $[Co_4(CO)_3(\mu_3\text{-}CO)_3(\mu_3\text{-}C_8H_8)(\eta^4\text{-}C_6H_8)]$ **2**, $[Co_4(CO)_5(\mu_3\text{-}CO)_3(\mu_3\text{-}C_8H_8)]$ **4**, the anions $[\mathbf{1}]^-$, $[\mathbf{2}]^-$, $[\mathbf{4}]^-$, the dianions $[\mathbf{1}]^{2-}$, $[\mathbf{2}]^{2-}$, $[\mathbf{4}]^{2-}$ and some related fragments, in particular the decapitation product of **1**–**4**, namely the anion $[Co_3(CO)_3(\mu\text{-}CO)_3(\mu_3\text{-}C_8H_8)]^-$ **5**, were performed using DFT calculations (details are given in the Experimental section). The agreement between the calculated and the available experimental structures (derived from X-ray crystallo-

Table 3 The composition (%) and energies (eV) of the HOMO and the LUMO of the cluster complexes $[Co_4(CO)_3(\mu_3\text{-}CO)_3(\mu_3\text{-}C_8H_8)L_2]$ **1**, $[\mathbf{1}]^-$ ($L_2 = \eta^4\text{-}C_8H_8$); **2**, $[\mathbf{2}]^-$ ($L_2 = \eta^4\text{-}C_6H_8$); **4**, $[\mathbf{4}]^-$ (L = CO) and $[Co_3(CO)_3(\mu\text{-}CO)_3(\mu_3\text{-}C_8H_8)]^-$ **5**. For atom numbering *cf.* Scheme 1

	1		$[\mathbf{1}]^-$		**2**		$[\mathbf{2}]^-$		**4**		$[\mathbf{4}]^-$		**5**	
Energy/eV	−328.9911		−331.4804		−312.4166		−314.4562		−260.3848		−262.7997		−223.3629	
	HOMO	LUMO	HOMO	LUMO	HOMO	LUMO	HOMO	LUMO	HOMO	LUMO	HOMO	LUMO	HOMO	LUMO
Energy/eV	−5.026	−3.838	−0.885	−0.339	−5.046	−3.539	−0.338	+0.306	−5.539	−4.011	−0.625	+0.001	−1.483	+0.694
Co1	14.87	23.90	21.40	37.69	9.55	28.03	28.50	31.88	5.56	29.21	30.16	30.11	—	—
Co2	21.66	2.78	2.62	2.66	25.57	16.42	15.82	18.74	42.39	21.22	21.43	20.42	3.14	23.08
Co3	22.31	3.91	2.32	2.58	22.94	15.62	15.10	17.66	11.13	12.68	12.16	14.50	36.30	13.75
Co4	3.86	12.52	12.16	15.84	7.43	1.89	1.18	0.96	6.90	6.09	4.20	4.31	36.36	13.59
Co2,Co3,Co4	47.83	19.52	17.10	21.09	55.94	33.93	32.10	37.36	60.42	39.99	37.79	39.23	75.80	50.42
η^1-CO	2.29	1.42	1.05	1.47	2.63	2.73	2.28	1.59	1.77	2.29	2.62	2.57	2.43	10.10
μ-CO	8.71	4.44	3.28	3.91	14.22	4.40	4.83	4.35	13.85	7.55	7.31	10.44	4.89	5.41
$\mu_3\text{-}C_8H_8$	13.35	4.88	4.00	4.05	13.56	6.56	7.43	6.14	12.12	6.01	6.51	4.65	14.82	28.91
L_2	6.32	37.84	41.96	24.47	0.36	16.51	18.22	10.49	0.47	8.92	8.77	8.31	—	—
Co1–L_2	21.29	61.74	63.36	62.16	9.91	44.54	46.72	42.37	6.03	38.13	38.93	38.42	—	—

graphy) is quite good. A comparison of experimental and calculated structural parameters is compiled in the Supplementary Material (Table S1). †

The nature of the frontier orbitals of the cluster complexes **1**, $[\mathbf{1}]^-$, **2**, $[\mathbf{2}]^-$, **4**, $[\mathbf{4}]^-$ and **5** was investigated. The composition and energies of the HOMO and LUMO of these complexes, as well as their relative energies are summarised in Table 3.

The cluster complexes have many common features, most importantly the $Co_3(CO)_3(\mu\text{-}CO)_3(\mu_3\text{-}C_8H_8)$ base, which constitutes, as the anion, the decapitation product **5**. The tetranuclear species can be constructed from **5** by adding an 'apical' CoL_2 fragment (Co1, $L_2 = \eta^4$-coordinated ring or two carbonyls) to the 'basal' tricobalt triangle (Co2Co3Co4, Scheme 1). Looking

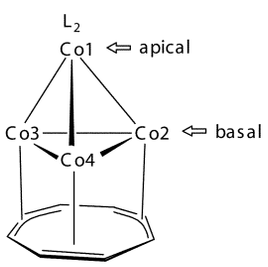

Scheme 1

at the series of tetranuclear μ_3-cyclooctatetraene complexes $[Co_4(CO)_3(\mu_3\text{-}CO)_3(\mu_3\text{-}C_8H_8)L_2]$ we note that in **1** ($L_2 = \eta^4\text{-}C_8H_8$) the HOMO is mainly concentrated on three cobalts (one Co atom of the 'basal' triangle is not contributing much) and the μ_3-cot ring, while in **2** ($L_2 = \eta^4\text{-}C_6H_8$) it is less localized on Co1 and more on the bridging carbonyls. This tendency is increased in the octacarbonyl complex **4** (L = CO), with a negligible contribution of Co1 and a larger one of Co4, the μ_3-ring, and the bridging carbonyls to the HOMO.

The LUMOs of these species are very similar to the HOMOs of their anions, which are paramagnetic species. For cluster **1**, the strongest contributions to the LUMO come from the apical Co1 and the C_8H_8 ring attached to it in the tetrahapto fashion. Therefore, upon reduction, the extra electron becomes considerably localized in this part of the molecule. In the monoanion species $[\mathbf{1}]^-$, the spin density is mainly localised on Co1 (57%) and the basal Co4 (21%). Conversely, for the cluster **2** with the apical cyclohexadiene, the LUMO is a more delocalized orbital, with contributions from Co1 and the C_6H_8 ring, but also the basal Co2 and Co3. In the anion of cluster **2**, *i.e.* $[Co_4(CO)_3(\mu_3\text{-}CO)_3(\mu_3\text{-}C_8H_8)(\eta^4\text{-}C_6H_8)]^-$ $[\mathbf{2}]^-$, the spin density is essentially distributed among Co1, Co2, and Co3 (49%, 23% and 21%, respectively). The third cluster studied was the octacarbonyl derivative **4**, which has the LUMO essentially localized on Co1 and Co2. This is reflected in the spin density of the anion $[\mathbf{4}]^-$ (Co1 44%, Co2 33%, and Co3 16%, respectively). The LUMO of the trinuclear anion $[Co_3(CO)_3(\mu\text{-}CO)_3(\mu_3\text{-}C_8H_8)]^-$ **5** is well delocalised over the whole complex.

When the clusters are reduced, some structural parameters change, as can be seen in Table 4. The trend in Co–Co distances corresponds to a slight weakening of all the metal–metal bonds, both basal–basal and basal–apical. More interesting changes affect the apical CoL_2 moiety. In complex **1**, the distances from Co1 to the 1, 4 carbon atoms of the $\eta^4\text{-}C_8H_8$ ring ('outer' carbons of the η^4-diene moiety) increase significantly (2.30, 2.25 Å in **1** to 2.56, 2.49 Å in $[\mathbf{1}]^-$). The corresponding elongation of the distance to the 'inner' (2, 3) carbons is much less dramatic (2.02 Å in **1** as compared to 2.03 and 2.05 Å in $[\mathbf{1}]^-$). These changes in the cobalt–carbon distances indicate that the bonds of Co1 to the external diene carbons are becoming weaker, or, in other words, that there is a small haptotropic shift of the diene unit, tending toward a η^2-coordination mode (Fig. 4).

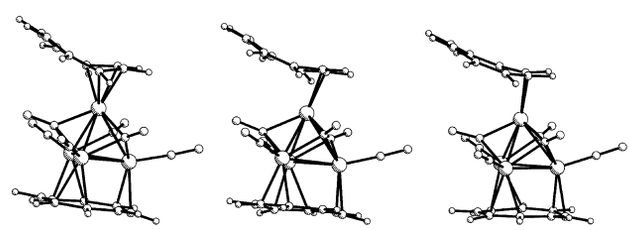

Fig. 4 Calculated structures showing the $\eta^4 \longrightarrow \eta^2$ ring slippage of the cot ring upon reduction of $[Co_4(CO)_3(\mu_3\text{-}CO)_3(\mu_3\text{-}C_8H_8)(\eta^4\text{-}C_8H_8)]$, **1** (left), to the anion $[\mathbf{1}]^-$ (centre) and the diamagnetic dianion $[\mathbf{1}]^{2-}$ (right).

Cluster **2**, $[Co_4(CO)_3(\mu_3\text{-}CO)_3(\mu_3\text{-}C_8H_8)(\eta^4\text{-}C_6H_8)]$, also has an η^4-coordinated ring, cyclohexadiene, in the apical position. However, compared to **1** reduction has a much smaller effect on the cobalt carbon distances involving this ring ('inner' diene carbons: from 2.03 Å in **2** to 2.06 Å in $[\mathbf{2}]^-$; 'outer' diene carbons: from 2.12 Å in **2** to 2.23 Å in $[\mathbf{2}]^-$). With respect to the Co1–C distances, the η^4-diene moiety in $[\mathbf{2}]^-$ compares well with the one in **2**.

The structures of the dianions $[\mathbf{1}]^{2-}$, $[\mathbf{2}]^{2-}$ and $[\mathbf{4}]^{2-}$, were fully optimised both as paramagnetic (triplet) and diamagnetic (low spin singlet) species. In any case, the diamagnetic dianion was found to be the more stable of the two alternatives (by 0.295 eV for $[\mathbf{1}]^{2-}$, 0.006 eV for $[\mathbf{2}]^{2-}$, and 0.698 eV for $[\mathbf{4}]^{2-}$ or 6.8, 0.14 and 16.1 kcal mol^{-1}, respectively).

Upon further reduction of $[\mathbf{1}]^-$ to the dianion $[\mathbf{1}]^{2-}$ the haptotropic shift of the apical cot ligand becomes more pronounced. The calculated Co1–C bond lengths of $[\mathbf{1}]^{2-}$ (Table 4) are now in accord with an essentially η^2-cot ligand, which becomes almost planar (Fig. 4). In marked contrast, the geometry of the apical Co1(cyclohexadiene) moiety in $[\mathbf{2}]^{2-}$ remains similar to

Table 4 Comparison between some calculated distances (Å) in the cluster complexes $[Co_4(CO)_3(\mu_3\text{-}CO)_3(\mu_3\text{-}C_8H_8)L_2]$ **1** ($L_2 = \eta^4\text{-}C_8H_8$), **2** ($L_2 = \eta^4\text{-}C_6H_8$), **4** (L = CO) and their corresponding anions $[\mathbf{1}]^-$, $[\mathbf{2}]^-$, $[\mathbf{4}]^-$, and dianions $[\mathbf{1}]^{2-}$, $[\mathbf{2}]^{2-}$, $[\mathbf{4}]^{2-}$. For atom numbering *cf.* Scheme 1

	1	$[\mathbf{1}]^-$	$[\mathbf{1}]^{2-}$	**2**	$[\mathbf{2}]^-$	$[\mathbf{2}]^{2-}$	**4**	$[\mathbf{4}]^-$	$[\mathbf{4}]^{2-}$
Co1–Co2	2.48	2.48	2.47	2.44	2.52	2.62	2.41	2.54	2.42
Co1–Co3	2.48	2.50	2.48	2.45	2.52	2.61	2.52	2.62	2.53
Co1–Co4	2.53	2.55	2.58	2.55	2.52	2.50	2.62	2.64	2.60
Co2–Co3	2.58	2.59	2.59	2.56	2.62	2.69	2.56	2.61	2.57
Co2–Co4	2.54	2.59	2.62	2.55	2.58	2.61	2.56	2.58	2.58
Co3–Co4	2.55	2.60	2.65	2.55	2.59	2.61	2.55	2.57	2.61
Co1–$(L)_2$	2.30[a]	2.05[a]	2.83[a]	2.12[a]	2.23[a]	2.29[a]	1.76	1.78	1.74
	2.02[b]	2.02[b]	2.06[b]	2.03[b]	2.06[b]	2.05[b]	1.78	1.79	1.76
	2.02[b]	2.02[b]	2.05[b]	2.03[b]	2.06[b]	2.05[b]			
	2.25[a]	2.49[a]	2.81[a]	2.12[a]	2.23[a]	2.28[a]			

[a] 'Outer' carbons of the 1,4-diene ligand. [b] 'Inner' carbons of the 1,4-diene ligand.

that in $[\mathbf{2}]^-$ and **2**. Most of the effects of the second reduction are seen in the Co_4 frame (further lengthening of Co–Co bonds, Table 4). Cluster **4**, $[Co_4(CO)_5(\mu_3\text{-}CO)_3(\mu_3\text{-}C_8H_8)]$, behaves differently. Indeed, the first electron leads to a weakening of the bonds in the Co_4 framework and the Co1–C bonds to the apical carbonyls. The Co–C bonds to the μ_3-cot remain the same (six bonds in the 2.08–2.22 Å range in **4**, 2.10–2.25 Å in $[\mathbf{4}]^-$; two bonds at 2.44, 2.45 Å in **4**, 2.47, 2.51 Å in $[\mathbf{4}]^-$; two bonds at 2.68, 2.69 Å in **4**, 2.67, 2.70 Å in $[\mathbf{4}]^-$; one non bonding distance, 2.92 in **4**, 2.93 Å in $[\mathbf{4}]^-$). The second electron induces a partial decomplexation of the μ_3-cot ring, which becomes non-planar and η^6-coordinated, with three cobalts eclipsing three double bonds of cot (six Co–C bonds between 2.09 and 2.20 Å, two non-bonding distances at 3.08, 3.10 Å) and all the other bonds become closer to those in **4** than those in $[\mathbf{4}]^-$ (Table 4, Fig. 5).

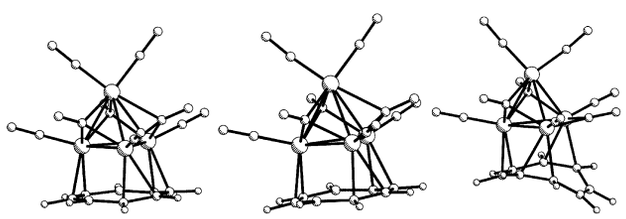

Fig. 5 Calculated structures showing the geometrical consequences of the reduction of $[Co_4(CO)_5(\mu_3\text{-}CO)_3(\mu_3\text{-}C_8H_8)]$ **4** (left), $[\mathbf{4}]^-$ (centre) and diamagnetic $[\mathbf{4}]^{2-}$ (right).

Discussion

Reduction of the complexes $[Co_4(CO)_3(\mu_3\text{-}CO)_3(\mu_3\text{-}C_8H_8)L_2]$ **1**–**3** proceeds in two subsequent reversible one-electron steps. The IR spectra during the first reduction show a bathochromic shift of the bands by 51–54 cm^{-1} for terminal CO and by 55–63 cm^{-1} for bridging CO stretches, evidently with little change in the general features of the spectra. The second reduction step causes a significantly larger shift of the terminal ν(CO) bands towards lower frequencies (by 59 cm^{-1} for $[\mathbf{2}]^- \longrightarrow [\mathbf{2}]^{2-}$ and 83 cm^{-1} for $[\mathbf{3}]^- \longrightarrow [\mathbf{3}]^{2-}$), and a smaller shift of the bridging ν(CO) bands (by 33 cm^{-1} for $[\mathbf{2}]^- \longrightarrow [\mathbf{2}]^{2-}$ and 53 cm^{-1} for $[\mathbf{3}]^- \longrightarrow [\mathbf{3}]^{2-}$). Although CO band shifts caused by reduction of a complex cluster system are not simply predictable, the trends seem to indicate that the first extra electron is somewhat localized on the apical CoL_2 moiety, whereas the second reduction also increases the charge on the basal tricobalt frame connected to the facial C_8H_8 ligand.

Our DFT calculations clearly show that the energy of the neutral cluster complexes **1**, **2** and **4** becomes more negative when an electron is added. This stabilization is 2.48 eV for **1**, 2.41 eV for **4**, and 2.04 eV for **2**, suggesting that the clusters which give the more stable anions will be more easily reduced. This correlates with the first reduction potentials (−0.68 V, −0.60 V and −1.02 V for **1**, **4** and **2**, respectively). The differences between **1** and **4** are very small, both in what concerns stabilization of the anion and the reduction potentials. The relative stabilization of the anions can be understood from the bonding. Notice that, besides the ligands changing from cluster to cluster, there is a fixed core with six carbonyls, accounting for their electron acceptor properties. Cluster **1**, $[Co_4(CO)_3(\mu_3\text{-}CO)_3(\mu_3\text{-}C_8H_8)(\eta^4\text{-}C_8H_8)]$, can accommodate the extra electron in a metal–ring antibonding orbital which loses part of this character by means of ring slippage, as described above, stabilizing the reduced cluster (Fig. 4). The behaviour of complex **4**, $[Co_4(CO)_5(\mu_3\text{-}CO)_3(\mu_3\text{-}C_8H_8)]$, is typical of carbonyl derivatives, as a result of their π-acceptor capability. The third cluster, **2**, $[Co_4(CO)_3(\mu_3\text{-}CO)_3(\mu_3\text{-}C_8H_8)(\eta^4\text{-}C_6H_8)]$, is a poorer electron acceptor, as it contains less carbonyls than **4**, and a ring which cannot easily undergo slippage.

Reductively induced ring slippage has been discussed extensively for odd-membered rings.[15] It results from the metal–ring antibonding nature of the LUMO of the species before reduction. Slippage helps to relieve such antibonding character, stabilizing this orbital and making the process energetically more favourable. As illustrated in Fig. 6 the HOMOs of

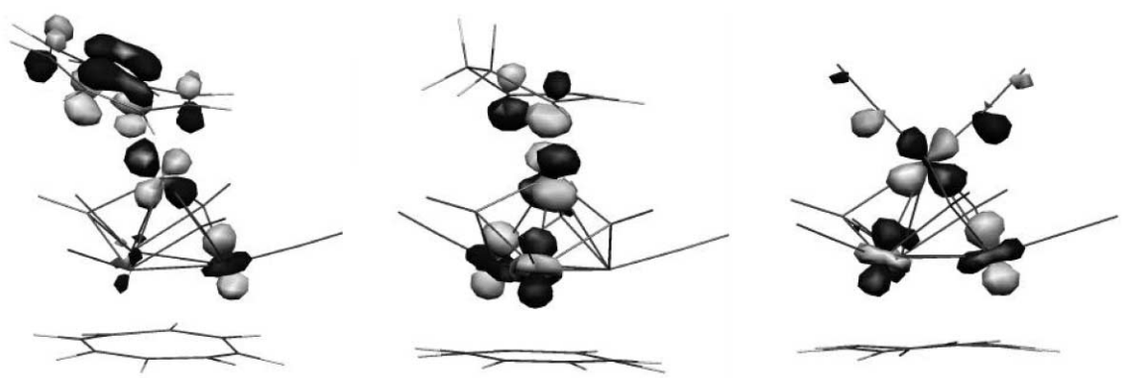

Fig. 6 3D representations of the HOMO of the complexes $[Co_4(CO)_6(C_8H_8)_2]^-$ $[\mathbf{1}]^-$ (left), $[Co_4(CO)_6(C_8H_8)(C_6H_8)]^-$ $[\mathbf{2}]^-$ (centre) and $[Co_4(CO)_8(C_8H_8)]^-$ $[\mathbf{4}]^-$ (right).

the reduced clusters **1**, **2** and **4** posses the same nature. The LUMOs of mononuclear complexes containing the Co(η^4-C_8H_8) fragment are also similar.[16] For example, an analysis of the ESR spectra of the 19 valence electron complexes [(η-C_5H_5)Co(1,2,3,4-η-C_8H_8)]$^-$ and [(η-C_6Me_6)Co(1,2,3,4-η-C_8H_8)] showed the SOMOs to be highly delocalized on the cyclooctatetraene ring, with about 40% and 50%, respectively, metal-d character.[16b]

In cluster **1**, [$Co_4(CO)_3(\mu_3$-$CO)_3(\mu_3$-$C_8H_8)(\eta^4$-$C_8H_8)$], slippage of the apical ring upon reduction is also driven by the tendency to decrease the antibonding character of the LUMO of the cluster (the HOMO of the anion [**1**]$^-$), as reflected in the new Co1–C distances. It should be added that in [**1**]$^-$ all the carbon atoms of the diene moiety are still within bonding distance of the apical cobalt atom, so that the hapticity might be described as intermediate between η^4 and η^2 (Scheme 2; a, b). Slipping

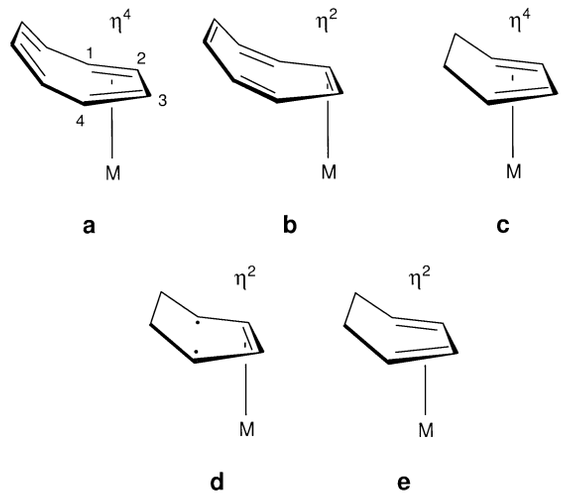

Scheme 2

towards the η^2-coordination becomes pronounced in [**1**]$^{2-}$. Such effects have been similarly observed for the addition of one electron to a five-membered ring, the elongation of the M–C bonds being smaller than the one observed upon addition of two electrons.[17]

In complex **2**, a similar slippage of the apical cyclohexadiene ligand is expected to be less favourable (Scheme 2; c, d) since the ring acquires some biradical character. Another possible structure involves significant reorientation of the six membered ring (Scheme 2; e). The full optimization of the anions [**2**]$^-$ and [**2**]$^{2-}$ shows that the best structural option does not involve much slippage of the cyclohexadiene ring, but causes only weakening of Co1–C and Co–Co bonds, resulting from the antibonding character of the HOMO.

The calculated energy minimum for the dianion of the octacarbonyl derivative, [**4**]$^{2-}$, is characterized by an η^2:η^2:η^2 coordination of the facial cot ligand. Such a coordination geometry, where only six of the eight ring carbons take part in bonding to the metal cluster, has been found experimentally in the trinuclear alkylidyne bridged complex [$Co_3(CO)_6$-(μ_3-CPh)(μ_3-cot)], which has the same skeletal electron count as [**4**]$^{2-}$.[18]

In any case, the compositions of the LUMOs of the clusters **1**, **2** and **4** are similar to those of the HOMOs of their anions and support the idea that the first extra electron is strongly located in the "head" of the cluster, the apical $Co1L_2$ fragment (Table 4). This finding correlates well with the observed changes of the ν(CO) bands during reduction, as discussed above. While in **2** and **4** the metal contributes more than the apical ligand(s) L_2, this does not apply to cluster **1**, where the apical C_8H_8 ring accounts for the highest contribution. The Co1–L_2 antibonding character is easily seen in the pictures of the HOMOs of the three anionic clusters shown in Fig. 6.

Our spectroelectrochemical results clearly show that decapitation of **1**–**3** to give the trinuclear anion [$Co_3(CO)_6(C_8H_8)$]$^-$ **5** takes place after the first reductive electron transfer. This is reflected in the properties of the HOMO of the anions. The antibonding character between Co1 and the triangular group Co2, Co3, Co4 is obvious from Fig. 6. As expected from the formation of the final reduction product **5**, the bonding between the basal cobalt triangle and the face-capping C_8H_8 ring barely changes upon one-electron reduction of the tetranuclear clusters.

The degradation of the tetranuclear cobalt clusters **1**–**4** to give a trinuclear anion is not without precedence. A similar reaction has been observed during the chemical reduction of [$Co_4(CO)_{12}$].[19] However, this degradation reaction is difficult to stop at the trinuclear stage, and the corresponding product [$Co_3(CO)_{10}$]$^-$ is quite unstable, especially in the presence of a donor solvent like THF. In contrast, [$Co_3(CO)_6(C_8H_8)$]$^-$ **5** is a much more stable entity, and constitutes the single end-point of the reductive degradation pathway of the μ_3-cot bridged tetracobalt clusters. In fact, all complexes studied produce this tricobalt anion in almost quantitative yields upon strong chemical reduction or in the long timescale of exhaustive electrolysis. Obviously, the face-capping cyclooctatetraene ligand is responsible for this great stabilization of the tricobalt frame.

Comparing the two consecutive one-electron reductions of **1**–**4** we note that evidently, while energy is gained from the first reduction of the neutral cluster complexes, the second reduction step does not lead to further stabilization. While a singlet spin state is expected to be preferred for the dianions with apical cot and carbonyl ligands, the energy difference between the singlet and triplet isomers is very small for [**2**]$^{2-}$. However, the similar redox behaviour it exhibits suggests the formation of the same type of dianion. The formation of the diamagnetic dianionic species results in an increasing concentration of electron density in the same parts of the molecule affected by the first electron, with even higher antibonding Co1–L_2 and Co1–Co2,3,4 character. The loss of the Co1–L_2 fragment appears likely on these grounds.

In order to assess the decapitation process, the binding energy of each $Co1L_2$ fragment to the basal frame of the cluster was evaluated for two of the clusters and their anions. Using the fragment decomposition available in the ADF programme, binding energies between the anion **5** (the final reduction product) and appropriately charged CoL_2 fragments were calculated. Upon reduction, the binding energy drops from 6.8 to 3.02 eV for **1**, and from 7.1 to 3.7 eV for **2**. The weakening of this interaction between fragments could in principle reflect the tendency of the bonds between Co1 and the triangular cluster comprised of Co2, Co3 and Co4 to break.

Conclusions

In all the complexes studied, reduction eventually induces decapitation of the tetranuclear cluster to give a common trinuclear final product, [$Co_3(CO)_3(\mu$-$CO)_3(\mu_3$-$C_8H_8)$]$^-$ **5**. However, our electrochemical investigations prove a considerable lifetime of the primary tetranuclear reduction products [$Co_4(CO)_3(\mu_3$-$CO)_3(\mu_3$-$C_8H_8)L_2$]$^-$, and the formation of less long-lived dianions [$Co_4(CO)_3(\mu_3$-$CO)_3(\mu_3$-$C_8H_8)L_2$]$^{2-}$. This can be rationalized by the DFT calculations, which show the energies of the monoanions to be lower than those of the neutral clusters. The singly occupied HOMO is considerably localized in the head of the cluster, causing the geometry changes to strongly depend upon the apical ligand(s) (L_2). Different effects are found, which become even more visible upon the second reduction: haptotropic shifts of the apical cot ligand, a general weakening of the bonding between the cluster and the apical cyclohexadiene, or, in the absence of a suitable apical ligand, even a partial decomplexation of the facial cot. In any case, while stabilizing the reduced species, the calculated distortions

are not relevant for the formation of the final product **5**, which can be traced to a weakening of the Co_{apical}–Co_{basal} bonds ubiquitously present in the tetranuclear anions.

Acknowledgements

J. F., C. N. and D. O. acknowledge support by EC-COST D15 program (grant D15/0001/99, and STSM financial assistance to J. F.), MURST (Rome) (COFIN-99) and the University of Torino ("scambi culturali"). Thanks are due to PRAXIS XXI for a Ph.D. grant to S. S. M. C. G. (BD 3805/96). R. M. and H. W. thank the Deutsche Forschungsgemeinschaft for support. A joint travel grant by the Deutscher Akademischer Austauschdienst, Conselho de Reitores Universidades Portuguesas and Instituto de Cooperação Científica e Tecnologia Internacional ("Acções Integradas Luso-Alemãs", A-10/01) to M. J. C. and H. W. is gratefully acknowledged.

References and notes

1 (*a*) W. E. Geiger, *Prog. Inorg. Chem.*, 1985, **33**, 275; (*b*) P. Zanello, *Struct. Bonding*, 1992, **79**, 101; (*c*) H. Vahrenkamp, in *The Synergy Between Dynamics and Reactivity at Clusters and Surfaces*, L. J. Farrugia, ed., *NATO ASI Series C: Mathematical and Physical Sciences*, Kluwer, Dordrecht, 1995, vol. 465, p. 297.
2 (*a*) R. P. Aggarval, N. G. Connelly, M. C. Crespo, B. J. Dunne, P. M. Hopkins and A. G. Orpen, *J. Chem. Soc., Dalton Trans.*, 1992, 655; (*b*) D. Osella, L. Milone, C. Nervi and M. Ravera, *Eur. J. Inorg. Chem.*, 1998, 1473.
3 H. Wadepohl, *Coord. Chem. Rev.*, 1999, **185–186**, 551.
4 H. Wadepohl, S. Gebert, R. Merkel and H. Pritzkow, *Eur. J. Inorg. Chem.*, 2000, 783.
5 H. Wadepohl, S. Gebert, H. Pritzkow, D. Osella, C. Nervi and J. Fiedler, *Eur. J. Inorg. Chem.*, 2000, 1833.
6 Throughout this paper, the face of the Co_4 cluster which binds the μ_3-C_8H_8, ligand will be referred to as the 'basal Co_3 plane' (*i.e.* Co2, Co3 and Co4). The forth cobalt (Co1, and the ligand(s) associated with it) is 'apical'; *cf.* Scheme 1.
7 H. Wadepohl, S. Gebert, H. Pritzkow, F. Grepioni and D. Braga, *Chem. Eur. J.*, 1998, **4**, 279.
8 M. Krejcik, M. Danek and F. Hartl, *J. Electroanal. Chem.*, 1991, **317**, 179.
9 R. G. Parr and W. Young, *Density Functional Theory of Atoms and Molecules*, Oxford University Press, New York, 1989.
10 ADF1999, E. J. Baerends, A. Bérces, C. Bo, P. M. Boerrigter, L. Cavallo, L. Deng, R. M. Dickson, D. E. Ellis, L. Fan, T. H. Fischer, C. Fonseca Guerra, S. J. A. van Gisbergen, J. A. Groeneveld, O. V. Gritsenko, F. E. Harris, P. van den Hoek, H. Jacobsen, G. van Kessel, F. Kootstra, E. van Lenthe, V. P. Osinga, P. H. T. Philipsen, D. Post, C. C. Pye, W. Ravenek, P. Ros, P. R. T. Schipper, G. Schreckenbach, J. G. Snijders, M. Sola, D. Swerhone, G. te Velde, P. Vernooijs, L. Versluis, O. Visser, E. van Wezenbeek, G. Wiesenekker, S. K. Wolff, T. K. Woo and T. Ziegler, Vrije Universiteit, Amsterdam, The Netherlands, 1999.
11 S. H. Vosko, L. Wilk and M. Nusair, *Can. J. Phys.*, 1980, **58**, 1200.
12 (*a*) L. Versluis and T. Ziegler, *J. Chem. Phys.*, 1988, **88**, 322; (*b*) L. Fan and T. J. Ziegler, *Chem. Phys.*, 1991, **95**, 7401.
13 J. P. Perdew, J. A. Chevary, S. H. Vosko, K. A. Jackson, M. R. Pederson, D. J. Singh and C. Fiolhais, *Phys. Rev.*, 1992, **B46**, 6671.
14 S. Portmann and H. P. Lüthi, *Chimia*, 2000, **54**, 766.
15 M. J. Calhorda and L. F. Veiros, *Comments Inorg. Chem.*, 2001, **22**, 375.
16 (*a*) T. A. Albright, W. E. Geiger, Jr., J. Moraczewski and B. Tulyathan, *J. Am. Chem. Soc.*, 1981, **103**, 4787; (*b*) W. E. Geiger, Jr., P. H. Rieger, C. Corbato, J. Edwin, E. Fonsecca, G. A. Lane and J. M. Mevs, *J. Am. Chem. Soc.*, 1993, **115**, 2314.
17 M. E. Stoll, P. Belanzoni, M. J. Calhorda, M. G. B. Drew, V. Félix, W. E. Geiger, C. A. Gamelas, I. S. Gonçalves, C. C. Romão and L. F. Veiros, *J. Am. Chem. Soc.*, 2001, **123**, 10595.
18 (*a*) M. D. Brice, R. J. Dellaca, B. R. Penfold and J. L. Spencer, *J. Chem. Soc. D*, 1971, 72; (*b*) R. J. Dellaca and B. R. Penfold, *Inorg. Chem.*, 1972, **11**, 1855.
19 (*a*) G. Fachinetti, *J. Chem. Soc., Chem. Commun.*, 1979, 396; (*b*) H. N. Adams, G. Fachinetti and J. Strähle, *Angew. Chem.*, 1980, **92**, 411.